

Acknowledgment. This work was supported by a Grant-in-Aid for Scientific Research (Grant No. 02453089) and a Special Grant-in-Aid for Promotion of Education and Science in Hokkaido University from the Ministry of Education, Science and Culture, Japan. Partial financial support from Sapporo Bioscience Foundation is gratefully acknowledged.

Supplementary Material Available: Experimental details and spectroscopic data for **2a-g**, **3a-f**, **9a**, and **10a** (4 pages). Ordering information is given on any current masthead page.

Control of Back Electron Transfer from Charge-Transfer Ion Pairs by Zeolite Supercages

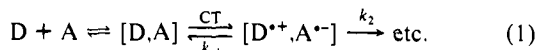
S. Sankararaman, K. B. Yoon, T. Yabe, and J. K. Kochi*

Department of Chemistry, University of Houston
University Park, Houston, Texas 77204-5641

Received October 5, 1990

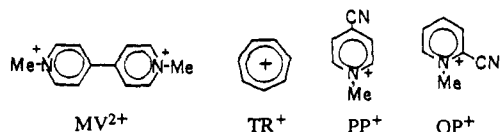
Revised Manuscript Received December 10, 1990

Charge-transfer activation of the precursor complexes¹ from nucleophiles (D) and electrophiles (A) is a viable formulation for a variety of organic and organometallic reactions, i.e.,



where CT includes both photochemical ($h\nu_{CT}$) and thermal (adiabatic) processes.² The critical assessment of charge-transfer efficiency depends largely on the rate of back electron transfer (k_{-1}) relative to that of the followup reaction (k_2), especially as evaluated in photoactivated systems.³ Since the available methodology for the general control of back electron transfer is limited,⁴ we describe in this report how the zeolite supercage can be used to strongly modulate the magnitude of k_{-1} .

The stepwise assembly of various charge-transfer complexes directly within the zeolite (Y) supercage has recently been achieved by the prior ion exchange of NaY with the different cationic electrophiles (A⁺) MV²⁺, TR⁺, PP⁺, and OP⁺ followed by exposure of the doped zeolite to arene donors (D = Ar) dissolved in organic solvents.⁵ Importantly the correlation of the



(1) See: (a) Mulliken, R. S.; Person, W. B. *Molecular Complexes: A Lecture and Reprint Volume*; Wiley: New York, 1969. (b) Kosower, E. M. *Adv. Phys. Org. Chem.* **1965**, *3*, 81.

(2) (a) Davidson, R. S. in *Molecular Association*; Foster, R., Ed.; Academic: New York, 1975; Vol. 1. (b) Davidson, R. S. *Adv. Phys. Org. Chem.* **1983**, *19*, 1. (c) Kochi, J. K. *Acta Chem. Scand.* **1990**, *44*, 409.

(3) Jones, G., II *Photoinduced Electron Transfer, Part A*; Fox, M. A., Chanon, M., Eds.; Elsevier: New York, 1989; p 245 ff.

(4) (a) Fox, M. A. *Adv. Photochem.* **1986**, *13*, 237. (b) Mataga, N.; Shioyama, H.; Kanda, Y. *J. Phys. Chem.* **1987**, *91*, 314.

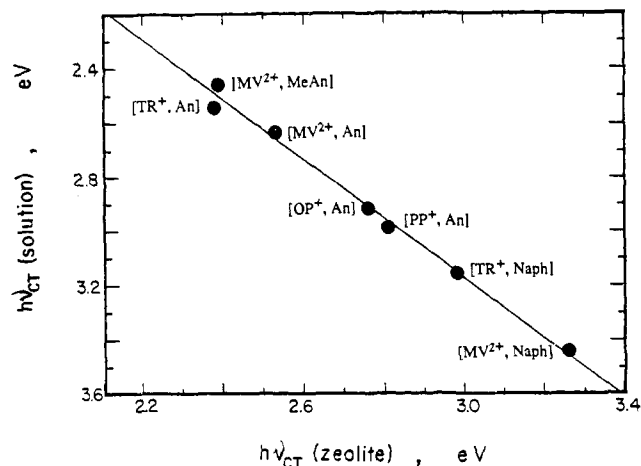


Figure 1. Charge-transfer spectra ($h\nu_{CT}$) of various charge-transfer complexes (as indicated) in zeolite-Y supercages by diffuse reflectance relative to the absorption spectra of the same complexes in acetonitrile solution.

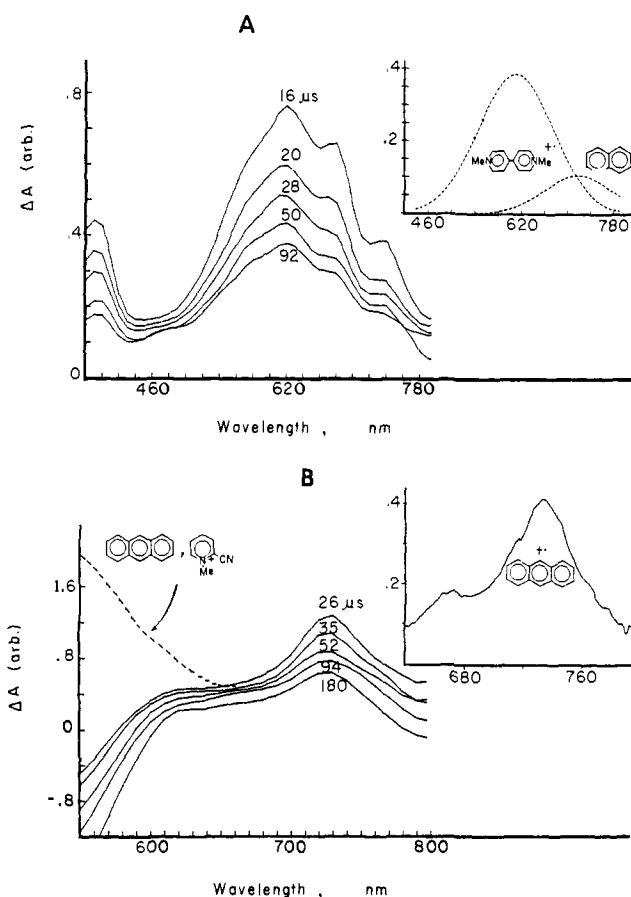


Figure 2. Time-resolved diffuse reflectance spectra obtained at microsecond intervals following the 10-ns laser pulse at (A) 355 nm of [MV²⁺, Naph] and (B) 532 nm of [OP⁺, An] immobilized in zeolite-Y. The insets show the transient spectra of the ion-radicals MV²⁺ (smoothed), Naph²⁺, and An²⁺ in acetonitrile solutions.

charge-transfer bands in Figure 1 establishes the intermolecular complexes [A⁺, Ar] that are formed within the zeolite-Y supercage to be the same as those produced in solution.⁶ Indeed the latter relate to the cofacial pairs of A⁺ and Ar in the π -complexes (established by X-ray crystallography⁷) that can be accommodated

(5) Yoon, K. B.; Kochi, J. K. *J. Am. Chem. Soc.* **1989**, *111*, 1128.

(6) See, e.g.: (a) Nakahara, A.; Wang, J. H. *J. Phys. Chem.* **1963**, *67*, 496. (b) Hamity, M.; Lema, R. H. *Can. J. Chem.* **1988**, *66*, 1552. (c) Atherton, S. J.; Hubig, S. M.; Callan, T. J.; Duncanson, J. A.; Snowden, P. T.; Rodgers, M. A. J. *J. Phys. Chem.* **1987**, *91*, 3717 and references therein.

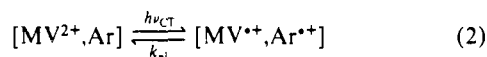
Table I. Spectral Decay of Charge-Transfer Ion Pairs in Zeolite-Y Supercages and in Acetonitrile Solution

Ar (E°_{ox}) ^a	A ⁺ (E°_{red}) ^b	zeolite		acetonitrile	
		λ_{CT}^c	$\tau,^d \mu s$	λ_{CT}^c	$\tau,^d ps$
Naph (1.62)	MV ²⁺ (-0.43)	380	6.8	~360	30
	C ₇ H ₇ ⁺ (-0.18)	415	3.3	393	25 ^f
	OP ⁺ (-0.62)	-	6.2	~330 ^e	-
	PP ⁺ (-0.64)	-	0.11	~330 ^e	25
An (1.41)	MV ²⁺	490	64	472	19
	C ₇ H ₇ ⁺	520	4.2	488	25 ^f
	OP ⁺	449	9.2	425	-
	PP ⁺	441	3.9	415	-
9-McC ₁₄ H ₉ (1.23)	MV ²⁺	518	5.6	504	28
	PP ⁺	-	-	439	27
9,10-Mc ₂ C ₁₄ H ₈ (1.09)	MV ²⁺	-	-	526	21
	PP ⁺	-	-	474	22

^aNaph = naphthalene, An = anthracene, C₁₄H₉ = anthracenyl, and C₁₄H₈ = anthracenediyl; oxidation potential in MeCN (V vs SCE). ^bMV²⁺ = methylviologen, C₇H₇⁺ = tropylium, OP⁺ = *N*-methyl-2-cyanopyridinium, and PP⁺ = *N*-methyl-4-cyanopyridinium; reduction potential in MeCN (V vs SCE). ^cCharge-transfer band maximum (nm). ^dLifetime as first-order decay. ^eUnresolved band. ^fFrom ref 16b.

within the zeolite-Y supercage.⁵

The deliberate photoexcitation of such immobilized CT complexes was initially carried out with a 10-ns (fwhm) pulse at 355 or 532 nm from a Nd³⁺:YAG laser, and the spectral transients were detected by the diffuse reflectance method of Kessler and Wilkinson.⁸ The typical time-resolved (difference) spectra in Figure 2 show (A) the simultaneous formation of the CT ion pair [MV²⁺,Naph^{•+}] from the naphthalene (Naph) complex with methylviologen (MV²⁺) and (B) the bleaching (negative ΔA) of the charge-transfer band (λ_{max} 490 nm) accompanying the production of the anthracene cation radical (An^{•+}, λ_{max} 725 nm) from the CT excitation of the *N*-methyl-2-cyanopyridinium complex with anthracene (An).⁹ In each case, the charge-transfer transients produced in zeolite-Y were identified by direct comparison of their spectra with the transient spectra of the same ion radicals previously produced in acetonitrile solution by either spectroelectrochemical or flash photolytic techniques.^{10,11} The gradual diminution of the transient spectrum shown in Figure 2 over a period of several microseconds corresponded to the mutual annihilation of the CT ion pairs by back electron transfer (k_{-1}), e.g.,



[Note that the control experiments established that the (CT) colored zeolites remained intact despite the steady-state irradiation of the charge-transfer bands for prolonged periods with monochromatic light.] For example, the kinetics analysis of the transient spectrum in Figure 2A, consisting of the simple superposition of the spectral bands of MV²⁺ and Naph^{•+} by Gaussian deconvolution, showed a homogeneous decay profile over the entire envelope from 540 to 740 nm. The lifetimes (τ) of the CT ion pairs thus produced within the zeolite supercage varied by roughly an

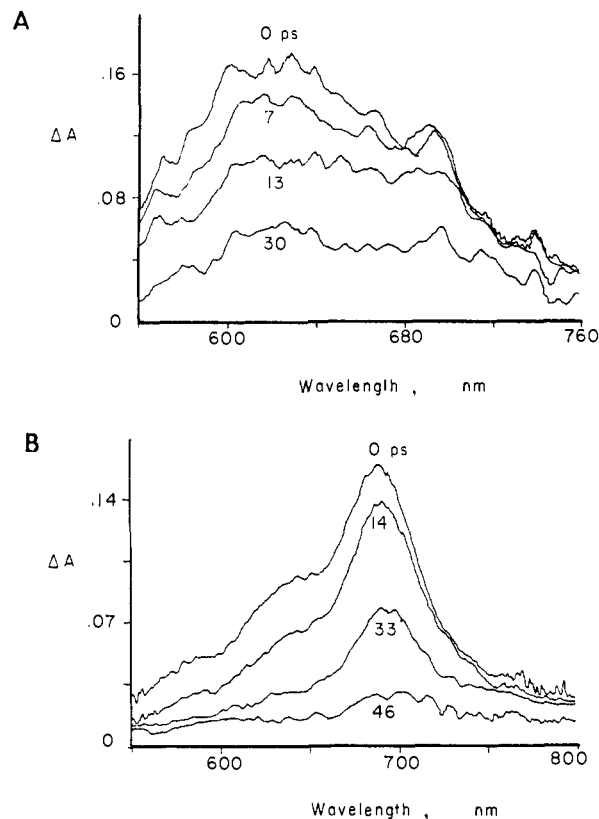


Figure 3. Time-resolved picosecond absorption spectra following the excitation of the CT complexes (A) [MV²⁺,Naph] and (B) [PP⁺,MeC₁₄H₉] in acetonitrile solutions with a 20-ps (fwhm) laser pulse.

order of magnitude between 0.11 and 9.2 μs among the various complexes listed in Table I.¹² The transient absorbance did not return completely to the base line,¹³ somewhat reminiscent of the decay previously observed from arene and carbonyl triplet states in zeolites.¹⁴

In strong contrast to the rather prolonged (microsecond) lifetimes of CT ion pairs produced within zeolite supercages, the laser flash photolysis of the same complexes generated in solution yielded spectral transients that could be detected only on the picosecond time scale. Thus Figure 3 shows the time-resolved picosecond spectra in the spectral region between 550 and 750 nm of (A) the CT ion pair [MV²⁺,Naph^{•+}] from the naphthalene complex with methylviologen and (B) the 9-methylanthracene cation radical from the corresponding complex with the *N*-methyl-4-cyanopyridinium acceptor following the application of the 20-ps (fwhm) pulse from a Nd³⁺:YAG laser. In all cases, the time-resolved picosecond spectrum in solution was the same as that observed in the zeolite supercage (vide supra). Most importantly, the short lifetimes of the CT ion pairs in solution, as given in Table I,¹² lie close to the temporal resolution of the laser-flash spectrometer, and they are in the range of those previously measured in solution for other systems^{15,16} with similar driving forces for back electron transfer. As such, the factor of 10⁵–10⁶ that prolongs the lifetimes of the CT ion pairs in the zeolite supercage (column 4) is sufficient to distinguish the strong environmental influences that modulate

(12) The absorbance decrease was treated as a first-order decay.

(13) For example, the minor residual absorbance (after ~100 μs) did not arise from a photoproduct since the intensity of the CT band in the zeolite was unchanged after irradiation (vide supra).

(14) Wilkinson, F.; Willsher, C. J.; Casel, H. L.; Johnston, L. J.; Scaiano, J. C. *Can. J. Chem.* **1986**, *64*, 539. See also ref 8.

(15) (a) Gould, I. R.; Moody, R.; Farid, S. *J. Am. Chem. Soc.* **1988**, *110*, 7242. (b) Asahi, T.; Mataga, N. *J. Phys. Chem.* **1989**, *93*, 6575.

(16) (a) Hilinski, E. F.; Masnovi, J. M.; Kochi, J. K.; Rentzepis, P. M. *J. Am. Chem. Soc.* **1984**, *106*, 8071. (b) Takahashi, Y.; Sankararaman, S.; Kochi, J. K. *J. Am. Chem. Soc.* **1989**, *111*, 2954. (c) Wallis, J. M.; Kochi, J. K. *J. Am. Chem. Soc.* **1988**, *110*, 8207. Thus the lifetimes listed in Table I (column 6) could represent the upper limits.

(7) Yoon, K. B.; Kochi, J. K. *J. Phys. Chem.*, in press.

(8) Kessler, R. W.; Wilkinson, F. *J. Chem. Soc., Faraday Trans. 1* **1981**, *77*, 309. See also: Willsher, C. J. *J. Photochem.* **1985**, *28*, 229. Wilkinson, F. *J. Chem. Soc., Faraday Trans. 1* **1986**, *82*, 2073. Wilkinson, F.; Willsher, C. J. *Tetrahedron* **1987**, *43*, 1197.

(9) The accompanying spectrum of the *N*-methyl-2-cyanopyridinyl radical occurs with λ_{max} in the region between 380 and 460 nm. See: Itoh, M.; Nagakura, S. *Bull. Chem. Soc. Jpn.* **1966**, *39*, 369.

(10) (a) Gschwind, R.; Haselbach, E. *Helv. Chim. Acta* **1979**, *97*, 941. (b) Steenken, S.; Warren, C. J.; Gilbert, B. C. *J. Chem. Soc., Perkin Trans. 2* **1990**, 335. (c) Badger, B.; Brocklehurst, B. *Trans. Faraday Soc.* **1969**, *65*, 2588. (d) Brocklehurst, B.; Russell, R. D. *Trans. Faraday Soc.* **1969**, *65*, 2159. (e) Badger, B.; Brocklehurst, B.; Russell, R. D. *Chem. Phys. Lett.* **1967**, *1*, 122.

the rate of back electron transfer relative to that in solution (column 6). Adsorption effects of ionic species at the polar aluminosilicate surface and/or the electrostatic field within the zeolite supercage^{17,18} could be the contributory factors in the marked retardation of the electron-transfer rate. Indeed from the magnitude of the latter, we estimate the CT ion pair to be stabilized within the zeolite supercage over that in solution by roughly 8 kcal mol⁻¹.^{19,20} The chemical consequences accompanying the dramatically prolonged lifetimes of CT ion pairs enabled by zeolite supercages will be reported at a later time.

Acknowledgment. We thank the National Science Foundation, Robert A. Welch Foundation, and Texas Advanced Research Program for financial support.

(17) (a) Rabo, J. A. *Catal. Rev. Sci. Eng.* **1981**, 23, 293. (b) Rabo, J. A. In *Zeolite Chemistry and Catalysis*; Rabo, J. A., Ed.; ACS Monograph 171; American Chemical Society: Washington, DC, 1976; p 332 ff. (c) Rabo, J. A.; Kasai, P. H. *Prog. Solid State Chem.* **1975**, 9, 1. Compare also: Ozin, G. A.; Gil, C. *Chem. Rev.* **1989**, 89, 1749. Rolison, D. R. *Chem. Rev.* **1990**, 90, 867.

(18) The same experiment on a wet zeolite afforded a transient spectrum that consisted only of that derived from MV^{•+} owing to the rapid hydration of Naph^{•+} (compare Steenken, S., et al. in ref 10b) at the wall. Furthermore, note the poor correlation between the driving force for back electron transfer $\mathcal{F} (E^{\circ}_{red} + E^{\circ}_{ox})$ and the lifetime ($-\log \tau$) of the CT ion pairs.

(19) Taken as the difference in the activation energies that are calculated from the k_{-1} ratios by cancellation of the preexponential terms in the zeolite and solution processes.

(20) For the behavior of other (uncharged) reactive intermediates in zeolites, see: (a) Turro, N. J. *Pure Appl. Chem.* **1986**, 58, 1219. (b) Wilkinson, F.; Willsher, C. J.; Leicester, P. A.; Barr, J. R. M.; Smith, M. J. C. *J. Chem. Soc., Chem. Commun.* **1986**, 1216. (c) Persaud, L.; Bard, A. J.; Campion, A.; Fox, M. A.; Mallouk, T. E.; Webber, S. E.; White, J. M. *J. Am. Chem. Soc.* **1987**, 109, 7309. (d) Krueger, J. S.; Mayer, J. E.; Mallouk, T. E. *J. Am. Chem. Soc.* **1988**, 110, 8232. (e) Corbin, D. R.; Eaton, D. F.; Ramamurthy, V. *J. Am. Chem. Soc.* **1988**, 110, 4848; *J. Org. Chem.* **1988**, 53, 5386. See also: Kalyanasundaram, K. *Photochemistry in Microheterogeneous Systems*; Academic: New York, 1987; p 317 ff. Fox, M. A., Ed. *Organic Transformations in Nonhomogeneous Media*; ACS Symposium Series 278; American Chemical Society: Washington, DC, 1985.

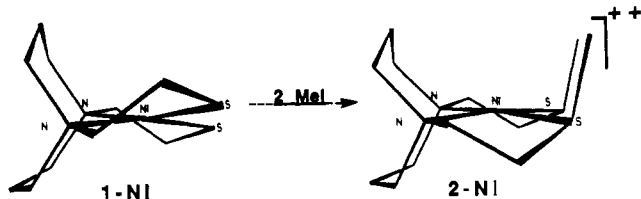
Applications of the N₂S₂ Ligand, N,N'-Bis(mercaptoethyl)-1,5-diazacyclooctane, toward the Formation of Bi- and Heterometallics: [(BME-DACO)Fe]₂ and [(BME-DACO)NiFeCl₂]₂

Daniel K. Mills, Yui May Hsiao, Patrick J. Farmer, Earl V. Atnip, Joseph H. Reibenspies, and Marcetta Y. Darensbourg*

Department of Chemistry, Texas A&M University
College Station, Texas 77843

Received October 5, 1990

Recently we reported the synthesis of a new macrocyclic ligand based on a derivative of diazacyclooctane, N,N'-bis(mercaptoethyl)-1,5-diazacyclooctane, H₂BME-DACO.¹ The X-ray crystal structures of the complexes (BME-DACO)Ni^{II} (1-Ni) and [(Me₂BME-DACO)Ni^{II}][I]₂ (2-Ni) were the first determined for



the N₂S₂ Busch-type² complexes as monomers, a success presumably due to the control of aggregation provided by steric bulk

(1) Mills, D. K.; Reibenspies, J. H.; Darensbourg, M. Y. *Inorg. Chem.* **1990**, 29, 4364.

(2) Busch, D. H.; Burke, J. A., Jr.; Jicha, D. C.; Thompson, M. C.; Morris, M. L. *Adv. Chem. Ser.* **1963**, No. 37, 125.

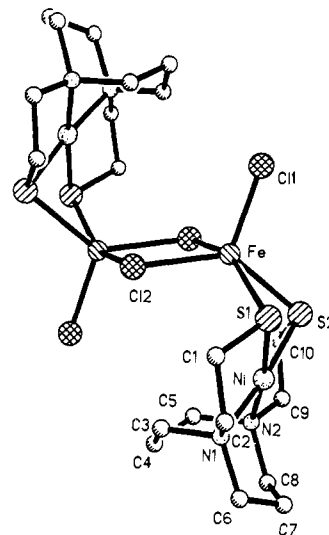


Figure 1. Molecular structure of [(BME-DACO)NiFeCl₂]₂ (1-Ni₂Fe₂). Selected bond lengths (Å): Fe-Cl(1), 2.286 (3); Fe-Cl(2), 2.422 (3); Fe-Cl(2A), 2.547 (3); Fe-S(1), 2.552 (3); Fe-S(2), 2.462 (3); Ni-S(1), 2.172 (3); Ni-S(2), 2.165 (3); Ni-N(1), 1.974 (8); Ni-N(2), 1.966 (9). Selected bond angles (deg): S(1)-Fe-Cl(2A), 153.6 (1); Cl(2)-Fe-S(2), 134.3 (1); Cl(1)-Fe-Cl(2A), 99.4 (1); Cl(1)-Fe-Cl(2), 111.9 (1); Cl(1)-Fe-S(1), 106.2 (1); Cl(1)-Fe-S(2), 113.7 (1); S(1)-Fe-S(2), 72.2 (1); Cl(2)-Fe-S(1), 93.1 (1); Cl(2)-Fe-Cl(2A), 82.9 (1); S(2)-Fe-Cl(2A), 91.9 (1); S(1)-Ni-S(2), 85.9 (1); Ni(1)-Ni(2), 91.0 (3); S(2)-Ni-N(2), 91.0 (2); S(1)-Ni-N(1), 91.3 (3); Ni-S(1)-Fe, 81.6 (1); Ni-S(2)-Fe, 83.9 (1); Fe-Cl(2)-Fe(A), 97.1 (1).

of the ligand. The structures evidenced the well-known conformational requirements of the DACO ring,³ resulting in a sterically protected hydrophobic pocket, especially for the 2-Ni complex, where dialkylation occurred on the same side of the square plane.¹ This methylated derivative (and others alkylated with C₂H₅I, C₆H₅CH₂Br, *i*-C₃H₇I, and BrCH₂CH₂CH₂Br)⁴ results from the reactivity of the metal-bound thiolate sulfur atoms of 1-Ni analogous to that of the Busch-type (H₂NCH₂CH₂S)₂Ni^{II} complexes.⁵ In fact, the sulfurs in such complexes are potential binding sites for an additional metal as illustrated by [(H₂NC-CH₂CH₂)₄Ni₃](I)₂.² Structural studies by Dahl and Wei showed the trimetallic to consist of three linked square planes: two NiN₂S₂ planes separated by a NiS₄ plane at torsional angles of 109°. ⁶

We are applying the ability of 1-Ni to serve as a complex ligand toward the preparation of Ni and Fe heterometallics in biological-type ligation settings appropriate to provide redox and magnetic behavior for comparison to nickel-containing hydrogenases.⁷ To our knowledge [(BME-DACO)Ni(μ-Cl)FeCl₂]₂ (1-Ni₂Fe₂) is the first Ni/Fe heterometallic complex with classical (as opposed to organometallic) donor atoms and represents a new type of heterotetrametallic, containing two square-planar nickel(II) and two pseudo-square-pyramidal iron(II) ions. Square-pyramidal iron is also seen in [(BME-DACO)Fe]₂ (1-Fe₂) in which the iron(II) centers are simultaneously bound to two BME-DACO ligands, resulting in a 2Fe-2S core, analogous to the dimeric iron complex of dimethyl-N,N'-bis(2-mercaptoethyl)-1,3-propanediamine, BME-Me₂PDA.⁸

Reaction of 1-Ni in CH₃CN with anhydrous FeCl₂ in either 2:1 or 1:1 molar equivalents results in formation of a thermally

(3) Broderick, W. E.; Jordan, R. F.; Kanamori, K.; Legg, J. I.; Willet, R. D. *J. Am. Chem. Soc.* **1986**, 108, 7122. Fecher, B.; Elias, H. *Inorg. Chim. Acta* **1990**, 168, 179, and references therein.

(4) Farmer, P. J.; Mills, D. K.; Darensbourg, M. Y. Unpublished results.

(5) Busch, D. H.; Jicha, D. C.; Thompson, M. C.; Wrathall, J. W.; Blinn, E. *J. Am. Chem. Soc.* **1964**, 86, 3642. Jicha, D. C.; Busch, D. H. *Inorg. Chem.* **1962**, 1, 872.

(6) Wei, C. H.; Dahl, L. F. *Inorg. Chem.* **1970**, 9, 1878.

(7) *The Bioinorganic Chemistry of Nickel*; Lancaster, J. R., Jr., Ed.; VCH Publishers, Inc.: New York, 1988.

(8) Karlin, K. D.; Lippard, S. J. *J. Am. Chem. Soc.* **1976**, 98, 6951. Hu, W. J.; Lippard, S. J. *J. Am. Chem. Soc.* **1974**, 96, 2366.